

Dynamic and Tensile Properties of Epoxy Resins

D. H. KAELBLE, *Central Research Laboratory, Minnesota Mining and Manufacturing Company, St. Paul, Minnesota*

Synopsis

The dynamic mechanical and tensile deformation and ultimate properties are reported for two epoxy resins in the temperature range, from the glass transition T_g to $T_g + 100^\circ\text{C}$. The epoxy resins are stoichiometrically reacted diglycidyl ether of bisphenol A with an aromatic ($T_g = 115^\circ\text{C}$.) and an aliphatic ($T_g = 47^\circ\text{C}$.) diamine curing agent. Dynamic measurements were conducted on a rotating cantilever beam instrument over the frequency range from 0.01–100 cycles/sec. Tensile deformation and fracture characterization were obtained by constant rate of strain measurement at strain rates of 0.000445–0.445 sec.⁻¹. Both dynamic and tensile modulus data as well as ultimate stress and strain response superimpose by time and temperature reduction to form unified "master curves." The time or frequency shift factor a_T for both dynamic and tensile deformation and fracture properties follow the predictions of the familiar Williams-Landel-Ferry equation. The rheological and fracture master curves are discussed in terms of both monomer composition and equilibrium response of the crosslinked network. The regions of maximum dynamic dispersion are associated with rubbery state high elasticity tensile response for these epoxies and the magnitude of responses correlated.

Introduction

Selected epoxy resins have previously been examined by dynamic mechanical property measurement over broad ranges of frequency and temperature.¹ In general, the dynamic response for epoxy resins, below their softening temperature, is quite similar to that of other amorphous high polymers which exhibit a glass transition at elevated temperatures. As the dynamic measurement proceeds into the thermal softening or glass transition range, the influence of the cross-linked network structure becomes much more predominant. Above the temperature range of glass transition an apparent equilibrium modulus of elasticity is evident from the dynamic measurement. An agreement has been obtained between the temperature regions of major dynamic property change and apparent second-order or glass transition temperature T_g . It has also been demonstrated that the time-temperature reduced variables treatment is applicable to dynamic data in the glass transition range for epoxy resins.

A recent theory by T. L. Smith² treats the time- and temperature-dependent stress-strain properties of a viscoelastic high polymer undergoing tensile deformation at constant rate of strain. An extension of the above treatment by Smith³ demonstrates that it applies also in defining the time and temperature dependence of ultimate tensile stress and strain of GR-S

rubber measured also under conditions of constant rate of strain deformation. These methods are applicable for temperatures equivalent to or greater than T_g for the polymer examined.

The present study was undertaken to determine possible interrelations between dynamic and tensile properties of two typical crosslinked epoxies over equivalent ranges of time and temperature. Particular attention is devoted to the temperature range $T_g < T < T_g + 100$, where recent analytic definitions of fundamental polymer properties apply, such as the equation of Williams, Landel, and Ferry.⁴ Data obtained in this temperature range also permit comparison of epoxies to other high polymers.

Experimental

The diglycidyl ether of bisphenol A was coreacted stoichiometrically with two diamine curing agents. The coreactants are characterized in Table I and formulation and curing conditions tabulated in Table II. Samples for dynamic testing, solid cylinders of approximately 0.250 in. diameter and 4.0 in. length, were either cast in glass tubes or machined from rectangular castings. Film castings of about 0.05 in. thickness were prepared for tensile testing. Taking advantage of the fact that these epoxies display rubberlike elasticity about 50°C. above T_g , miniature dumbbell specimens were hot-stamped from the heated sheets.

Dynamic property evaluation was carried out on the Maxwell device, a rotating cantilever beam instrument.⁵ This instrument, as presently developed in our laboratory, is described elsewhere.¹ The Maxwell device

TABLE I
Chemical Reactant

No.	Compound	Equivalent weight	Chemical structure
1	Diglycidyl ether of bisphenol A	200	
5	Methylene bis(o-chloroaniline)	66.5	
6	Aliphatic diamine	158	$\text{H}_2\text{NC}_{36}\text{H}_{63}\text{NH}_2$

TABLE II
Formulation and Curing Conditions

Cure recipe	Parts by weight		Cure conditions	
	Epoxy	Curative	Time, hr.	Temp., °C.
1-5	100	32.7	24	160
1-6	100	79	24	R.T.
			16	120

measures independently both the elastic (storage) and viscous (loss) contributions to total stiffness. These measurements are converted to storage modulus E_1 and loss modulus E_2 as described by the following relation for dynamic Young's modulus, E_R :

$$E_R = E_1 + iE_2 \quad (1)$$

and loss tangent ($\tan \delta$)

$$\tan \delta = E_2/E_1 \quad (2)$$

where δ is the phase angle between the sinusoidal stress and strain waves. The measurement results are discussed in terms of storage modulus, E_1 , and loss tangent, $\tan \delta$.

The Instron tensile tester (Instron Engineering Corp., Canton, Mass.) equipped with a Missimers temperature control cabinet (Missimers Inc., Los Angeles, Calif.) was utilized in conducting the tensile tests. The miniature dumbbell samples of 0.125 in. width, were compression-clamped in the Instron jaws with an effective gage length of 0.75 in. The jaw separation was set to permit the jaw line to occur on a slightly larger cross section located in the curved portion of the dumbbell specimen. This procedure eliminated jaw line failure in the data reported here and produced only a slight systematic (not more than 5%) difference between true strain in the uniform necked section and apparent strain as measured by jaw separation. Tests at each temperature were conducted at strain rates, $\dot{R} = \gamma/t$, which include 0.445, 0.0445, 0.00445, and 0.000445 sec.⁻¹ which correspond to crosshead speeds of 20.0, 2.0, 0.2, and 0.02 in./min., respectively. The tensile strength is reported in terms of the true stress at failure S_b , based on reduced cross-section area, and the ultimate strain γ_b , the ratio of length change to initial length (% elongation = $\gamma \times 100$).

From a point-slope analysis of tensile curves a first approximation to a time dependent relaxation modulus E_t was calculated by modifying the Smith equation.³

$$E_t = (S_r/\gamma_r) (d \log S_r/d \log \gamma_r) \quad (3)$$

in the following manner:

$$E_t \simeq (S_{r,t}/\gamma_{r,t}) (\log (S_{r,t}/S_{r,t-\Delta t})/\log(\gamma_{r,t}/\gamma_{r,t-\Delta t})) \quad (4)$$

where $S_r = S/R$ is the rate-reduced true stress and $\gamma_r = \gamma/R$ the rate-reduced strain. The tensile curves were analyzed by evaluating the reduced stress and reduced strain increments where $\gamma = 0.01, 0.02, 0.05, 0.10, 0.20, 0.50$, etc. From eq. (4), at $\gamma = 0.02$ the reduced stress and strain become $S_{r,t}$, and $\gamma_{r,t}$; at $\gamma = 0.01$ reduced stress and strain become $S_{r,t-\Delta t}$ and $\gamma_{r,t-\Delta t}$. This represents the first step of a series of increment analysis of each tensile curve where the strains (γ) associated with each step are indicated in Table III.

Use of a high speed digital computer for automatic computation and data-processing purposes greatly streamlines the experimental effort. This

TABLE III
Curve Analysis for First Approximation to Tensile Relaxation Modulus E_t

Step no.	Strain associated with $\gamma_{r,t}$	Strain associated with $\gamma_{r,t-\Delta t}$
1	0.02	0.01
2	0.05	0.02
3	0.10	0.05
4	0.20	0.10
5	0.50	0.20
6	1.00	0.50

method is applied to both dynamic and tensile measurements, as, for example, eq. (4) calculations. This technique permits application of the reduced variables method for data superposition, discussed in a later section, with practically no increased research effort.

Results

The dynamic mechanical properties of the aromatic diamine (cure 1-5) and aliphatic diamine (cure 1-6) cross-linked epoxy resins are graphically represented in Figures 1 and 2, respectively. The storage modulus E_1 and loss tangent ($\tan \delta$) are presented on three-dimensional plots as functions of frequency and temperature. The use of solid dots and dashed curves indicates one is viewing a reverse surface. The data cover a four-decade frequency range from 0.01 to 100 cycles/sec. and temperatures from -50°C . to above the softening region of the resins.

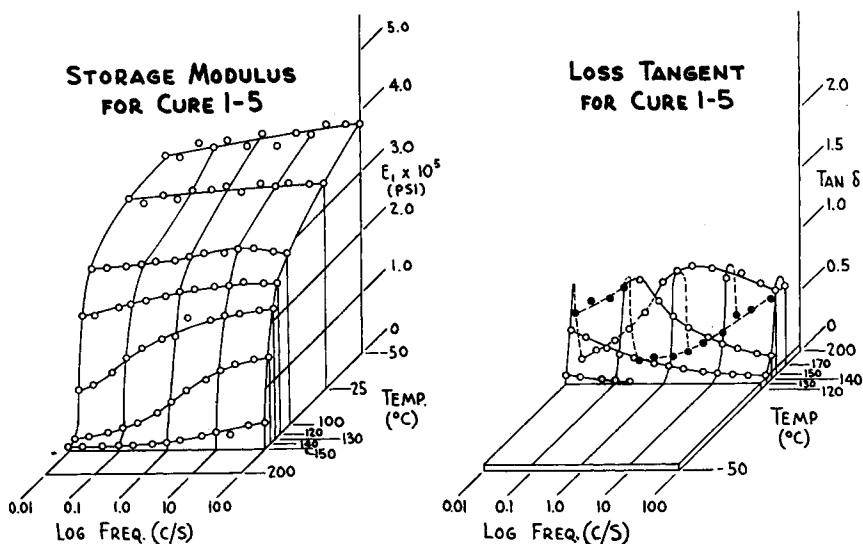


Fig. 1. Dynamic response surfaces (E_1 and $\tan \delta$) of an aromatic diamine-cured epoxy (cure 1-5).

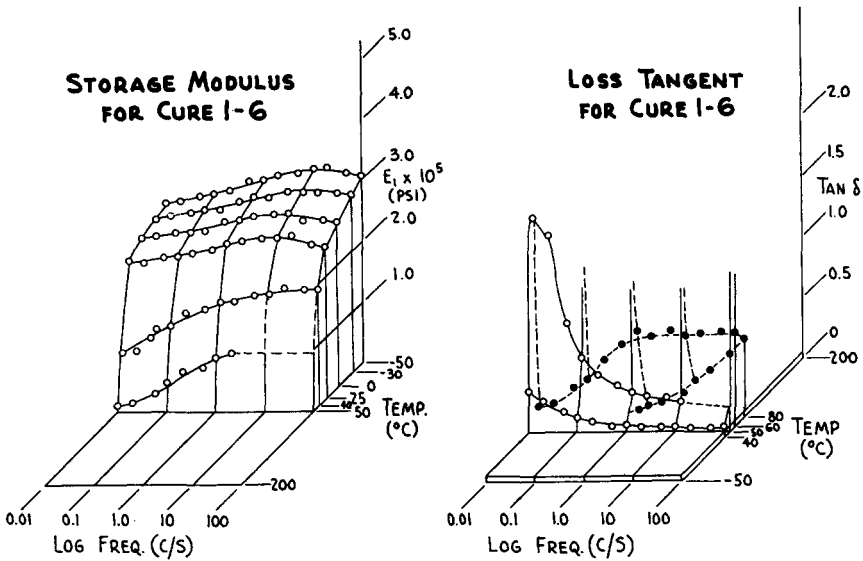


Fig. 2. Dynamic response surfaces (E_1 and $\tan \delta$) of an aliphatic diamine-cured epoxy (cure 1-6).

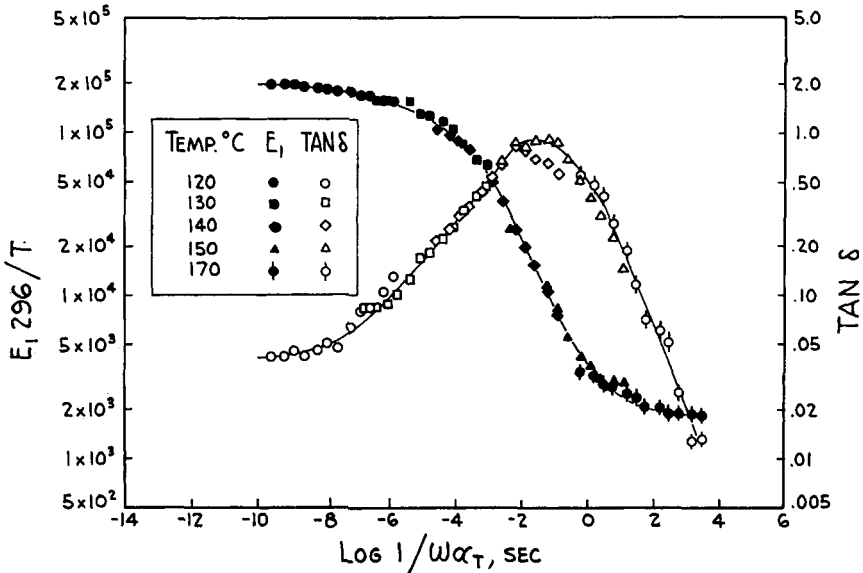


Fig. 3. Master curves of dynamic properties for cure 1-5.

From -50°C. to the softening regions for both cures 1-5 and 1-6 the dynamic data provide no evidence for a glassy state dispersion region as recognized by Deutch⁶ and Hoff⁷ for acrylic resins and previously recognized for an epoxy of the general type studied here.¹ A glassy state dynamic dispersion is associated with the "unfreezing" of a specific molecular mo-

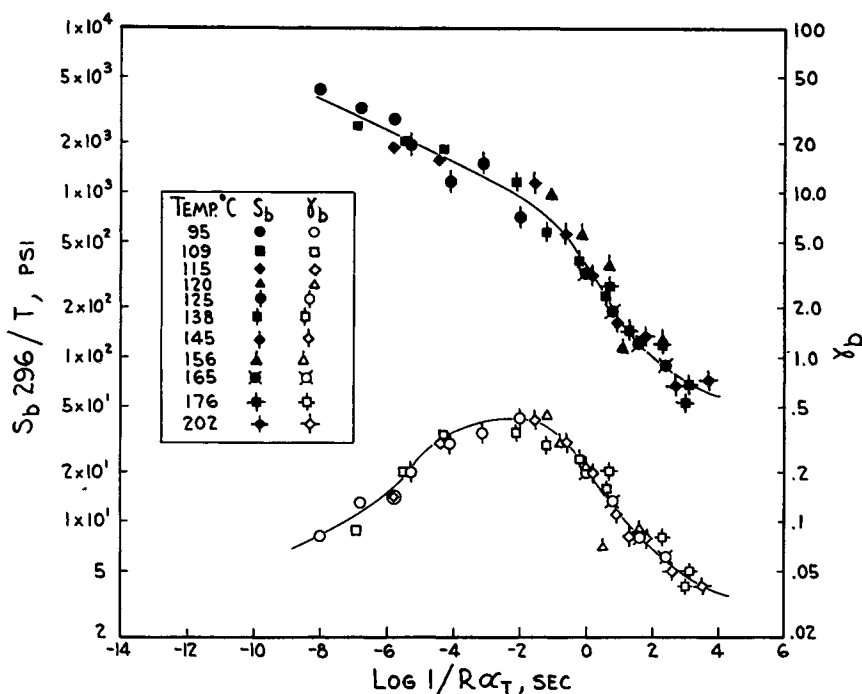


Fig. 4. Master curves of ultimate tensile properties (S_b and γ_b) for cure 1-5.

bility, such as a side group, and produces a slight decrease in E_1 and $\tan \delta$ maximum over a narrow frequency range.

Both cure 1-5 and cure 1-6 display typical glass transition dynamic dispersions; E_1 values decrease by factors of 100 to 1000, and $\tan \delta$ displays a major maximum over broad temperature and frequency ranges. Dynamic property change in the glass transition region is generally ascribed to a continuous unfreezing of a spectrum of molecular mobilities which produces a much broadened dispersion region. The temperature-frequency interdependence of properties in this region is evident from Figures 1 and 2.

Recent re-examination of the glass transition temperature by volume dilatometry, using a mercury confining liquid, produces values of $T_g = 115^\circ\text{C}$. for cure 1-5 and $T_g = 47^\circ\text{C}$. for cure 1-6. These dilatometric T_g values are in close agreement with previously reported¹ heat distortion temperatures of 119 and 47°C . for cure 1-5 and cure 1-6, respectively (by ASTM D648-45T at 264 outer fiber stress).

The principle of time-temperature superposition, applicable in the glass transition region, permits representation of data from several temperatures on a master curve referred to a single temperature. This technique is applied here to both dynamic and tensile property data. As suggested by previous convention,⁸ dynamic and tensile property master curves may be directly compared on an equivalent time base by plotting reduced reciprocal frequency $1/\omega a_T$ and reciprocal unit strain rate $1/Ra_T$. The

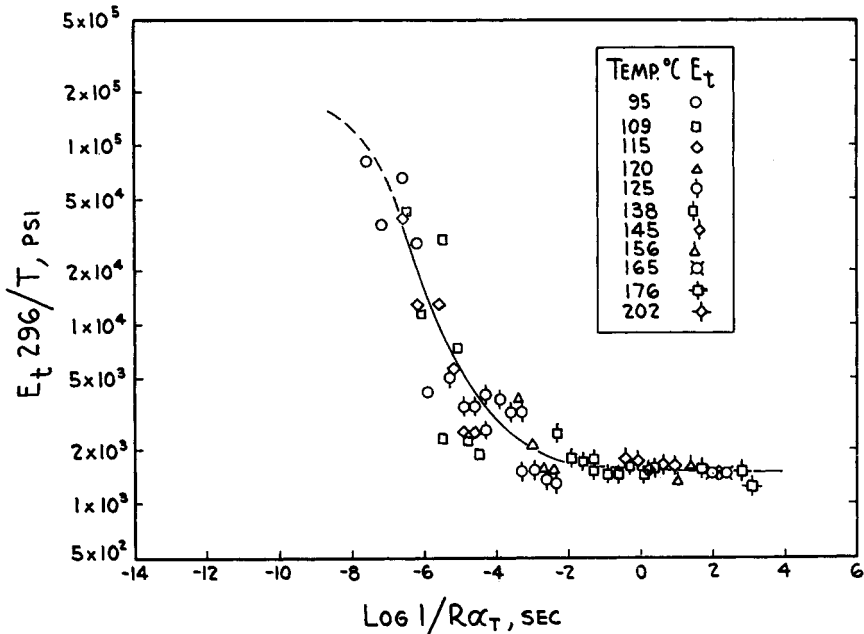


Fig. 5. Master curve of tensile relaxation modulus (E_t) for cure 1-5.

reference temperature T_s at which a_T , the time-temperature shift, becomes zero is chosen to be $T_g + 50^\circ\text{C}$. for both epoxies. Thus $T_s = 438^\circ\text{K}$. for cure 1-5 and for Cure 1-6, $T_s = 370^\circ\text{K}$. This reference temperature, defined by the WLF equation⁴

$$\log a_T = -8.86(T - T_s)/(101.8 + T - T_s) \quad (5)$$

where $T_s = T_g + 50$, provides a convenient means of comparing data between the two epoxies on a common reduced time scale. While both dynamic and tensile property curves are superimposed by using experimentally determined a_T values, comparison to the WLF function is conveniently available. To provide a common temperature base for reducing E_1 , E_t , and S_b magnitudes for the two epoxies in proportion to the absolute temperature, as required by the kinetic theory of elasticity, 23°C . is chosen and the temperature ratio $296/T$ applied where T is the test temperature (absolute).

The master curves of dynamic properties for cure 1-5 are presented in Figure 3. The E_1 function exhibits a smooth transition from glassy state values of about 2.0×10^5 psi to an approach toward a minimum equilibrium value of about 1.8×10^3 psi. In the dispersion region the $\tan \delta$ values display a maximum of about 0.90.

The ultimate tensile properties, S_b and γ_b , master curves for cure 1-5 are presented in Figure 4. The reasonable scatter of data is due in large part to recognized lack of reproducibility in ultimate property data. The ultimate stress function clearly displays a monotonic decrease in S_b with in-

creased failure time $1/Ra_T$. The ultimate strain function displays a maximum γ_b of about 0.40 in the transition region. A maximum range in γ_b has been reported by Smith for GR-S in the glass transition range.³

Figure 5 presents the tensile relaxation modulus master curve, as obtained from E_t values calculated by eq. (4). While scatter is displayed in the E

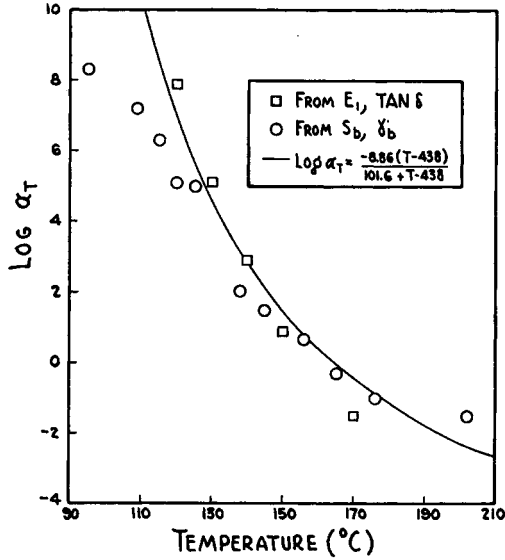


Fig. 6. Experimental values of a_T compared with predictions of WLF equation for cure 1-5.

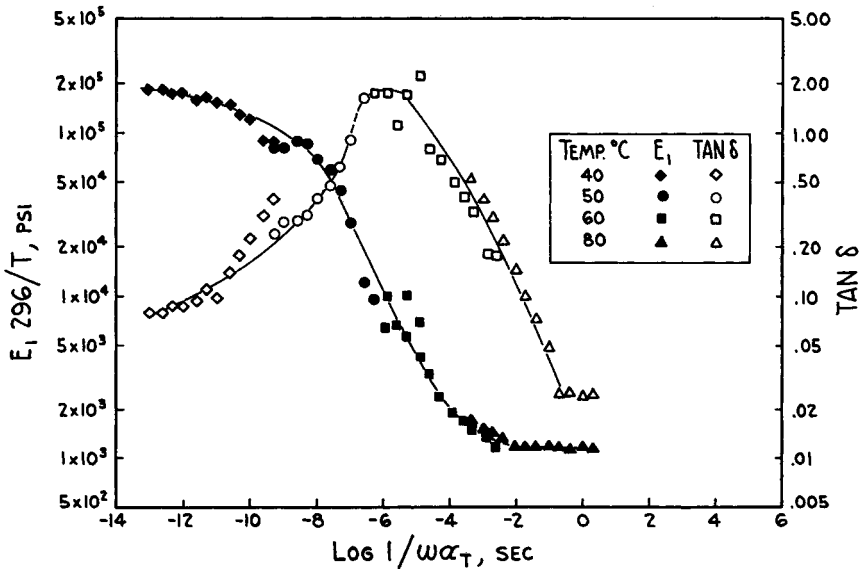


Fig. 7. Master curves of dynamic properties for cure 1-6.

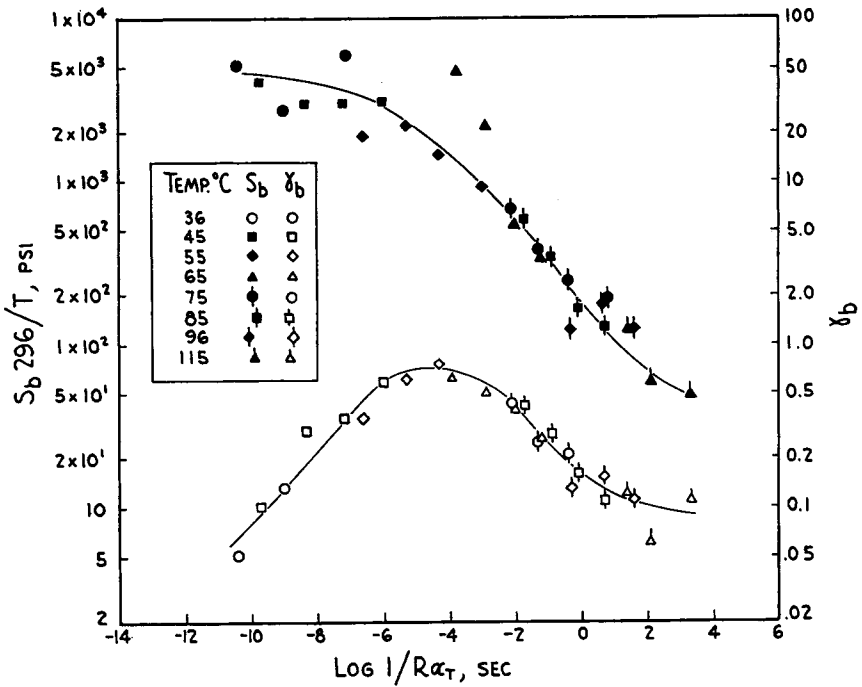


Fig. 8. Master curves of ultimate tensile properties (S_b and γ_b) for cure 1-6.

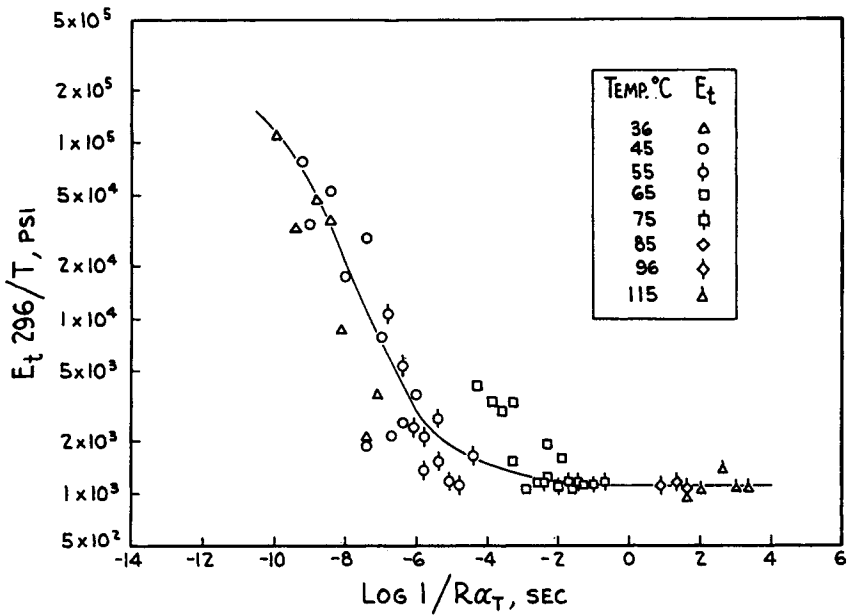


Fig. 9. Master curve of tensile relaxation modulus (E_t) for cure 1-6.

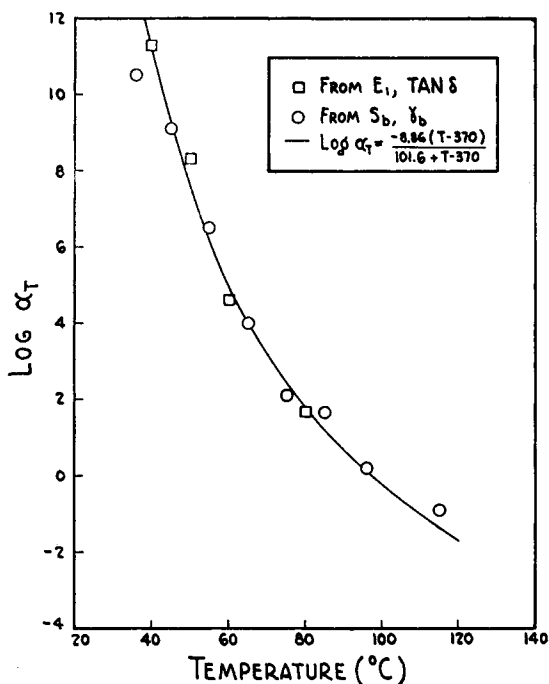


Fig. 10. Experimental values of a_T compared with predictions of WLF equation for cure 1-6.

data at low $1/Ra_T$ values, a broad region of equilibrium E_t values of about 1.6×10^3 psi magnitude is evident. The general similarity of the E_t function of Figure 5 and E_1 function of Figure 3 may be noted with a close agreement with the apparent equilibrium modulus values.

In Figure 6 are plotted the experimental a_T values from dynamic and tensile property data in comparison with the WLF function. The experimental a_T values exhibit reasonable agreement between the tensile and dynamic a_T factors and conform to the WLF function. The deviation of experimental a_T values obtained below T_g to values less than predicted by the WLF equation is in agreement with previous observations.⁴

The dynamic property master curves for cure 1-6, the aliphatic diamine-cured epoxy, are presented in Figure 7. The E_1 and $\tan \delta$ functions display close similarity in shape to similar curves for cure 1-5 presented in Figure 3. Differences of note are the lower magnitude of apparent equilibrium E_1 values, about 1.15×10^3 , and a higher dispersion region $\tan \delta$ maximum of approximately 1.8.

Ultimate tensile property data for cure 1-6, presented in Figure 8, again exhibit the regular decrease in S_b upon increasing $1/Ra_T$ values and a maximum in the γ_b function in the transition region. The ultimate strain in this region of maximum values is about 0.70 and recognizably higher than equivalent maximum values for cure 1-5.

The tensile relaxation modulus function for cure 1-6, shown in Figure 9, is practically coincident, neglecting data scatter, with the dynamic storage modulus function shown in Figure 6. The apparent equilibrium E_t value for cure 1-6 is 1.10×10^8 psi, again in close agreement with the equilibrium value from E_1 data.

Very good agreement between a_T values from dynamic and tensile data are apparent from Figure 10. An excellent fit of the experimental data to the WLF function is also evident. These data further evidence that the WLF equation may be realistically applied to both dynamic and tensile response data of thermosetting resins in the temperature region T_g to $T_g + 100^\circ\text{C}$.

Discussion

A few salient features of the dynamic and tensile property master curves are tabulated in Table IV. The demonstrated similarity between the storage modulus E_1 and tensile relaxation modulus E_t master curves for cures 1-5 and 1-6 is probably not fortuitous. It has been demonstrated on both a theoretical and experimental basis that provided a material displays linear viscoelasticity these master functions should be approximately equivalent.^{8,9} The agreement between the a_T factors obtained from dynamic data obtained at low strain ($\gamma < 0.002$) and ultimate tensile properties at high strains ($0.01 < \gamma < \gamma_b$) conforms with the prediction of the theory of Bueche¹⁰ which treats the tensile properties of polymers above T_g .

TABLE IV
Some Features of the Glass Transition Range Dynamic and Tensile Properties

	Cure 1-5	Cure 1-6
Maximum $\tan \delta$	0.90	1.80
Maximum γ_s	0.40	0.70
Equilibrium E_1 , psi	1800	1150
Equilibrium E_t , psi	1600	1100

If one assumes the equilibrium modulus values, E_1 and E_t , for cure 1-5 and cure 1-6 reflect only response of the crosslinked network a weight-average molecular weight between crosslinks, \bar{M}_c , may be calculated from (5):¹¹

$$\bar{M}_c = 3\rho RT/E \quad (5)$$

From Table IV, taking the average equilibrium modulus for cure 1-5 as $E = 1700$ psi with $\rho = 1.22$ g./cc. we calculate $\bar{M}_c = 770$. For cure 1-6, taking $E = 1150$ psi and $\rho = 1.06$ g./cc. the resulting value is $\bar{M}_c = 1020$. Assuming complete reaction of two moles of epoxy monomer with one mole of the diamine curatives described in Table I by idealized crosslinking, one may calculate an $\bar{M}_c = 365$ for cure 1-5 and $\bar{M}_c = 458$ for cure 1-6. Correlative information is presently lacking to support the calculated \bar{M}_c values from equilibrium modulus data. With the known complications

arising from steric and entanglement contributions to equilibrium E values these calculated \bar{M}_c values must be considered of relative significance.

Referring again to Table IV, one may note the aforementioned rather direct relative magnitudes of maximum $\tan \delta$ and γ_b values between cure 1-5 and cure 1-6. These values are also in regular inverse proportion to the equilibrium E values. It has been previously shown that maximum $\tan \delta$ values in the transition region of thermoset resins diminish with increased crosslinking.¹² The fact that both $\tan \delta$ and γ_b functions for the same crosslinked epoxy exhibit maxima in similar time regions suggests a close relation between these parameters.

The magnitudes of T_g for cure 1-5 and cure 1-6, from tensile, dynamic, and expansivity measurements, are in agreement with considerations of both cohesive energy density and main chain stiffness factors as they apply to amorphous high polymers.¹⁸ Previous studies have indicated that T_g in thermosetting resins depends upon the density of crosslinks.¹²

The demonstrated agreement of the experimental a_T values with the WLF function suggests fundamental similarities between these epoxies and amorphous high polymers as a class of material. The constants of the WLF equation are based upon the fractional free volume at the glass transition temperature and the coefficient of thermal expansion.⁴ The amenability of both dynamic and tensile data to the reduced variables treatment indicates linear viscoelasticity to high strains and configurational elasticity typical of other amorphous high polymers above T_g . The appearance of an equilibrium modulus in both tensile and dynamic data is typical of crosslinked polymers and permits calculation of an effective \bar{M}_c between crosslinks.^{3,9}

Aside from the purely analytic value of dynamic and tensile properties master curves, as already discussed, these functions may be applied to predicting performance characteristics. From both tensile and dynamic property master curves and their associated temperature function of a_T properties may be predicted at response times far from the direct experimental time range. For example, Instron tensile data should be applicable in predicting either short-time impact properties or long-time creep and failure properties. These predictions are accurate, of course, only when physical effects, such as sample heating and stress wave distortion, are negligible, and the material is chemically stable. In addition, master curves may be converted by the reverse of time-temperature superposition to the three-dimensional time-temperature plots of the type shown in Figures 1 and 2 for both tensile and dynamic properties.

References

1. Kaelble, D. H., *SPE J.*, **15**, 1071 (1959).
2. Smith, T. L., *J. Polymer Sci.*, **20**, 89 (1956).
3. Smith, T. L., *J. Polymer Sci.*, **32**, 99 (1958).
4. Williams, M. L., R. F. Landel, and J. D. Ferry, *J. Am. Chem. Soc.*, **77**, 3701 (1955).
5. Maxwell, B., *ASTM Bull.*, No. 215, 76 (July 1956).

6. Deutch, K., E. A. W. Hoff, and W. Reddish, *J. Polymer Sci.*, **18**, 565 (1954).
7. Hoff, E. A. W., D. W. Robinson, and A. H. Willbourn, *J. Polymer Sci.*, **18**, 161 (1955).
8. Andrews, R. D., *Ind. Eng. Chem.*, **44**, 707 (1952).
9. Eirich, F. R., Ed., *Rheology*, Vol. 2, Academic Press, New York, Chap. 1.
10. Bueche, F., *J. Appl. Phys.*, **26**, 1133 (1955).
11. Treloar, L. R. G., *The Physics of Rubber Elasticity*, 2nd Ed., Clarendon Press, Oxford, 1958, p. 71.
12. Drumm, M. F., C. W. H. Dodge, and L. E. Nielsen, paper presented to the Division of Paint, Plastics and Printing Ink Chemistry, 127th Meeting American Chemical Society, April 1955; *Preprints*, **15**, No. 1, 257 (1955).
13. Mark, H., and A. V. Tobolsky, *Physical Chemistry of High Polymers*, Interscience, New York, 1950, p. 146.

Résumé

On décrit les propriétés mécaniques dynamiques, les propriétés de déformation en tension et de rupture pour deux résines époxy dans un domaine de températures allant depuis la température de transition vitreuse T_g jusqu'à $T_g + 100^\circ\text{C}$. Les résines époxy sont des éthers diglycidyliques du bisphénol-A ayant réagi avec une diamine aromatique ($T_g = 115^\circ\text{C}$) et une diamine aliphatique ($T_g = 47^\circ\text{C}$). Les mesures dynamiques ont été effectuées à des fréquences de 0.01 à 100 c/s. La déformation en tension et la mesure de la résistance au choc ont été obtenues à des vitesses d'élongation constantes variant pour chaque expérience de 0.000445 à 0.445 sec^{-1} . Les résultats du module dynamique et de tension ainsi que la force de rupture et la réponse à l'élongation forment par réduction du temps et de la température des "courbes principales" unifiées. La durée ou le facteur de glissement de fréquence (α_T) pour les déformations dynamiques et sous tension de même que les propriétés de rupture, suivent les prédictions de l'équation habituelle de Williams-Landel-Ferry. On discute des "courbes principales" rhéologiques et de rupture du point de vue de la composition en monomères et de la réponse de l'équilibre du réseau ponté. Les régions de dispersion dynamique maximum sont liées à la réponse en tension de l'état caoutchouteux fortement élastique de ces résines époxy et à la grandeur des réponses.

Zusammenfassung

Die dynamisch-mechanische und die Zugdeformation sowie die Reisseigenschaften zweier Epoxyharze im Temperaturbereich von der Glasumwandlungstemperatur T_g bis zu $T_g + 100^\circ\text{C}$ werden mitgeteilt. Die Epoxyharze sind stöchiometrische Reaktionsprodukte des Diglycidiläthers von Bisphenol-A mit einem aromatischen ($T_g = 115^\circ\text{C}$) und einem aliphatischen ($T_g = 47^\circ\text{C}$) Diaminhärter. Dynamische Messungen wurden mit einem Rotationsstabinstrument im Frequenzbereich von 0,01 bis 100 Hz ausgeführt. Zugdeformation und Bruchcharakterisierung wurden durch Messung bei konstanter Verformungsgeschwindigkeit zwischen 0,000445 und 0,445 sec^{-1} erhalten. Dynamische und Zugmodulerggebnisse sowie Reissspannung und Verformungsverhalten können durch Zeit-Temperaturreduktion zur Bildung von "Einheitskurven" superponiert werden. Der Zeit- oder Frequenzverschiebungsfaktor α_T folgt für dynamische und Zugverformung sowie für Brucheigenschaften den Voraussagen der bekannten Williams-Landel-Ferry-Gleichung. Die rheologischen und die Bruch-"Einheitskurven" werden in bezug auf Monomerzusammensetzung und Gleichgewichtsverhalten des Netzwerks diskutiert. Die Bereiche maximaler dynamischer Dispersion sind bei diesen Epoxyharzen mit einem kautschukartigen hochelastischen Zugverhalten verknüpft.

Received May 11, 1964